A RELAXATION METHOD FOR THE SOLUTION OF ROTATIONAL TRANSONIC NOZZLE FLOW

by

Thoralf Brecht

Thesis submitted to the Graduate Faculty of the
Virginia Polytechnic Institute and State University
in partial fulfillment of requirements for the degree of

MASTER OF SCIENCE

in

Mechanical Engineering

APPROVED:

E. F. Brown, Chairman

W. F. O'Brien

H. L. Moses

August, 1975

Blacksburg, Virginia

ACKNOWLEDGMENTS

This work was conducted under a research contract with the Douglas Aircraft Company. I would like to thank Mrs. Carolyn Flora for typing the manuscript and the Graphic Arts Department of the University's Media Services for preparing the figures.

I am thankful to Kevin E. Walsh for developing the fundamental program which was expanded as described in this thesis to include rotational flow. Dr. Joseph L. Steger's suggestion for modifying the definition of the potential function to include rotational flow is greatly appreciated.

Thanks are also due Professors Hal L. Moses and Walter F. O'Brien for their help. I am especially grateful to my advisor, Dr. Eugene F. Brown, for his advice and encouragement over the past year.

TABLE OF CONTENTS

LIST OF FIGURES

LIST OF TABLES

LIST OF SYMBOLS

A, B, C	Coefficients of the second derivatives in the governing equation
$\tilde{A}$	Coefficient matrix of governing equation in tridiagonal form
c	Speed of sound
C_D	Discharge coefficient
D	Non-homogeneous term in tridiagonal form of governing equation
F	A rotation function
$\tilde{f}$	Non-homogeneous vector in tridiagonal form of governing equation
G	A rotation function
ℓ	Number of iterations
L	Total length of constant-area section and nozzle
M	Mach number
$\dot{m}$	Mass flow rate
n	Coordinate normal to streamline
P	Pressure
r	Radial coordinate in the physical plane
R	Gas constant
R	Nozzle wall radius
R_i	Inner wall radius
R_o	Outer wall radius
s	Coordinate along streamline
S	Entropy
u	Axial velocity component

v	Radial velocity component
V	Velocity
w	Tangential velocity component
x	Axial coordinate in the physical plane
y	Lateral coordinate in the physical plane (for planar flow)
γ	Ratio of specific heats
Δx	Mesh spacing in axial direction (physical plane)
Δr	Mesh spacing in radial direction (physical plane)
$\Delta \xi$	Mesh spacing in axial direction (computational plane)
$\Delta \psi$	Mesh spacing in radial direction (computational plane)
θ	Flow angle
λ	Column underrelaxation factor
Λ	Nozzle relaxation factor
ξ	Axial coordinate in the computational plane
ρ	Density
ϕ	Velocity function
ϕ'	Potential function
$\tilde{\phi}$	Column vector of unknown ϕ's
ψ	Radial coordinate in the computational plane
Ψ	Steam function
ω	Rotation
$\frac{D}{Dt}$	Substantial derivative

Subscripts

c	Centerline or inner wall

i	Mesh point index in the axial direction (except when used with R)
imax	Largest axial index
j	Mesh point index in the radial direction
jmax	Radial index at outer wall
r	Radial derivative in the physical plane
th	Refers to outer wall at nozzle throat
x	Axial derivative in the physical plane
ξ	Axial derivative in the computational plane
ψ	Radial derivative in the computational plane
o	Stagnation conditions

Superscripts

*	Refers to sonic conditions
—	Average
~	Matrix or vector
^	Nondimensionalized quantity (appendix only)

1. INTRODUCTION

1.1 Problem Description

The exhaust nozzle is a critical component of a jet propulsion system. Its purpose is to create thrust by accelerating exhaust gases to a high speed. For the prediction of range, payload, and operating costs, accurate knowledge of exhaust nozzle performance is required. For example, studies of Mach 2.2 supersonic transport aircraft have shown that a 1% change in thrust coefficient results in a 2.4% change in specific fuel consumption, and a 3.1% change in operating costs (1). Thus accurate analytical evaluation of exhaust nozzle performance is essential for accurate prediction of aircraft performance.

Measurements indicate that gradients of total pressure and total temperature in an exhaust nozzle are large enough to have a significant effect on nozzle performance. Wehofer and Matz (2) tested several typical turbofan nozzle configurations with nonuniform inlet conditions and their tests showed that total pressure gradients could cause the discharge coefficient to vary up to 2% and the thrust coefficient to vary up to 3% from the values obtained with uniform inlet flow. Tests conducted with both total pressure and total temperature nonuniformities indicated that total temperature gradients could cause an additional 1% change in discharge coefficient and 3% change in thrust coefficient.

Gradients in stagnation properties are caused by processes which occur upstream of the nozzle itself. The mechanisms producing these nonuniformities include:

1. Radial dependence of energy input and extraction common in turbomachinery operation
2. Flow separation
3. Mixing of core and fan flow
4. Combustion and heat transfer
5. Frictional effects.

Not only must gradients in stagnation properties be accounted for, but also the problem is further complicated by its transonic nature. The total pressure is usually sufficient so that the flow downstream of the nozzle throat is supersonic. Thus any method of solution must be capable of solving such transonic flows.

1.2 Background

Several methods of solving transonic flow problems have been developed. Brown (1) and Walsh (3) present reviews of some of these methods. However, only a few of these methods pertain to rotational flow. Since rotation can be related to nonuniform stagnation properties by Crocco's theorem (4), consideration of rotational effects is equivalent to inclusion of the nonuniform effects mentioned in the preceding paragraph.

Ferri and Dash (5) used an indirect method to evaluate nozzle performance which included effects of gradients in stagnation conditions, viscosity, heat conduction, and non-constant specific heats. Their calculations which used a coarse grid show a 1 to 2% variation in jet impulse caused by flow nonuniformities. However indirect methods have a disadvantage in determining the performance of a specific nozzle in

that the method must be applied to a variety of velocity distributions until the desired wall shape is obtained.

Wehofer and Moger (6, 7) have developed a time-dependent method for the solution of rotational transonic nozzle flow problems. Their calculations show effects due to nonuniformities in stagnation conditions of up to 5% in discharge coefficients and of up to 7% in thrust coefficient. However, most time-dependent methods suffer the disadvantage of long computer time. Brown (1) indicates that relaxation methods may provide an order of magnitude improvement in computation time over that available with most time dependent methods.

Emmons (8) used relaxation methods in 1944 to solve transonic flow problems by hand calculations. However, because of stability problems, relaxation methods were unsuccessful in computerized calculations until Murman and Cole (9) in 1970 introduced type-dependent finite differencing, that is a differencing scheme which takes into account the local type of the governing equations. Since then other investigators have applied relaxation methods to solve the equations of motion expressed in terms of the potential function (linearized and non-linearized forms), the stream function, and the velocity components. However, few appplications of the relaxation method have been to internal flow problems. An exception is the work of Walsh (3) who applied the relaxation procedures of Jameson (10) and South and Jameson (11), which were successful for external flow, to irrotational flow within a nozzle. The work reported here is an extension of Walsh's work.

1.3 Formulation of the Governing Equations

The governing equations for inviscid compressible flow may be formulated in terms of the primitive variables, u and v, the stream function, Ψ, or the potential function, ϕ'. Since the equations of motion in terms of the primitive variables contain no second derivative terms, classical relaxation procedures cannot be directly applied. Bailey and Steger (12) used alternating forward and backward finite differences and a matrix modification to solve three-dimensional irrotational flow in terms of the velocity components. These primitive variables require more array area and more arithmetic per iteration than required by the use of the potential function or the stream function.

At first it would appear that the best way to solve a rotational axisymetric compressible flow problem would be to use the stream function. The relaxation process can then be applied to one second order equation in Ψ. However, the density also appears in the equation and is a double-valued function of the derivatives of Ψ. To determine the correct value of density it must be known whether the flow is subsonic or supersonic. Thus the character of the flow must be specified in advance and does not evolve naturally. Steger (13) used the stream function to solve external flow problems. Since it was necessary to control the solution with interactive graphics, Steger concluded that the stream function was not practical for computerized solutions.

The third common formulation of compressible flow problems is in terms of the potential function. The flow must be irrotational for the usual potential function to exist. Steger (14) suggested that the usual

definition of the potential function could be modified to include rotational flow. This retains the advantage of having one second-order equation to solve. A description of the modified potential equations is given in the next section.

2. METHOD DESCRIPTION

2.1 Governing Equations

In the absence of viscosity, heat conduction, and body forces, compressible fluid flow can be described by Euler's equation,

$$(\tilde{V} \cdot \nabla)\, \tilde{V} = -\frac{1}{\rho} \nabla P, \tag{2.1}$$

and the continuity equation,

$$\nabla \cdot (\rho \tilde{V}) = 0. \tag{2.2}$$

It is well known that for axially symmetric, steady, isentropic flow of an ideal gas, these equations can be simplified by use of the potential function, $\phi'(x,r)$, where ϕ' is defined by:

$$\frac{\partial \phi'}{\partial x} \equiv u$$

$$\frac{\partial \phi'}{\partial r} \equiv v.$$

The resulting equation of motion is

$$(c^2 - \phi_x'^2)\phi'_{xx} + (c^2 - \phi_r'^2)\phi'_{rr} - 2\phi'_x\, \phi'_r\, \phi'_{xr} + \frac{c^2}{r}\, \phi'_r = 0$$

where c, the sonic speed, is given in terms of the stagnation speed of sound, c_o, by

$$c^2 = c_o^{\,2} - \frac{\gamma-1}{2}\, (\phi_x'^2 + \phi_r'^2).$$

These equations which are valid only for irrotational flow were used by Walsh (3). They can be modified for application to rotational

flow (excluding the effects of viscosity, shocks, and thermal conductivity) by the introduction of two additional functions F(x,r) and G(x,r) and defining a velocity function, ϕ, such that

$$\phi_x + F \equiv u \tag{2.3}$$

$$\phi_r + G \equiv v \tag{2.4}$$

where u and v have been nondimensionalized with respect to the local stagnation speed of sound and x and r have been nondimensionalized with respect to the radius of the outer wall at the throat.

As is shown in Section 6.1.2, Eqs. 2.1 and 2.2 can be reduced to the nondimensional equation

$$\left[c^2 - (\phi_x + F)^2\right](\phi_{xx} + F_x) + \left[c^2 - (\phi_r + G)^2\right](\phi_{rr} + G_r) - (\phi_x + F)(\phi_r + G)(2\phi_{xr} + F_r + G_x) + \frac{c^2}{r}(\phi_r + G) = 0 \tag{2.5}$$

where

$$c^2 = 1 - \frac{\gamma-1}{2}\left[(\phi_x + F)^2 + (\phi_r + G)^2\right].$$

By differentiating Eq. 2.3 with respect to r and Eq. 2.4 with respect to x, the functions F and G can be related to the local rotation by

$$F_r - G_x = \omega$$

where

$$\omega \equiv \frac{\partial u}{\partial r} - \frac{\partial v}{\partial x}.$$

As is shown in Section 6.1.1, Crocco's theorem (4) can be used to find a relationship between ω and the radial variation of total pressure. It is given by

$$\omega = \frac{M_o/u}{M_o \gamma P_o} \left(1 - \frac{\gamma-1}{2} M_o^2\right) \frac{\partial P_o}{\partial r} . \tag{2.6}$$

In order to use Eq. 2.6 to determine ω, a knowledge of the total pressure at each point in the flow field is needed. Section 6.1.1 shows that for steady flow under the assumptions of negligible viscosity, body forces, and heat conduction, the total pressure is constant along a streamline, or equivalently,

$$\frac{DP_o}{Dt} = 0.$$

This fact is also noted by Wehofer and Moger (6).

For the purposes of symmetry and illustration both F and G were introduced into Eq. 2.5. However, there is no need to use both functions; either F or G may be eliminated with no loss of generality. Because G appears more frequently in Eq. 2.5 than F, G was eliminated. The governing equations then become:

$$\left[c^2 - (\phi_x + F)^2\right](\phi_{xx} + F_x) + \left[c^2 - \phi_r^2\right]\phi_{rr} - (\phi_x + F)\,\phi_r\,(2\phi_{xr} + F_r) + \frac{c^2}{r}\phi_r = 0 \tag{2.7}$$

$$c^2 = 1 - \frac{\gamma-1}{2}\left[(\phi_x + F)^2 + \phi_r^2\right]$$

$$F_r = \omega = \frac{M_o/u}{M_o\,\gamma P_o}\left(1 - \frac{\gamma-1}{2} M_o^2\right) \frac{\partial P_o}{\partial r} \tag{2.8}$$

$$\frac{DP_o}{Dt} = 0. \tag{2.9}$$

These equations are independent of the total temperature because nondimensionalization caused terms involving total temperature to cancel. Thus local Mach numbers and flow angles are independent of total temperature gradients. This result is confirmed by Ferri and Dash (5) and Taulbee and Boraas (15). However, this does not imply that performance coefficients are independent of total temperature gradients. Once a solution of the governing equations is obtained, total temperature gradients must be considered in the determination of the discharge coefficient and the thrust coefficient.

2.2 Coordinate Transformation

There are three reasons for using the coordinate transformation from the physical plane to a coordinate plane which is shown in Fig. 1. First, the transformation results in a rectangular computational grid, avoiding the complication of irregular finite difference molecules at the nozzle wall. Second, a computational plane of equally spaced mesh points provides greater accuracy than obtained by using unequal mesh spacings in the computational plane (16). Third, the coordinate transformation enhances stability in the supersonic region. This is because one axis of the computational plane is approximately aligned with the flow direction. Thus the backward finite difference, which is discussed in the next section, is also approximately aligned with the flow. Thus stability is maintained without the use of a rotated difference scheme in the supersonic region such as used by South and Jameson (11).

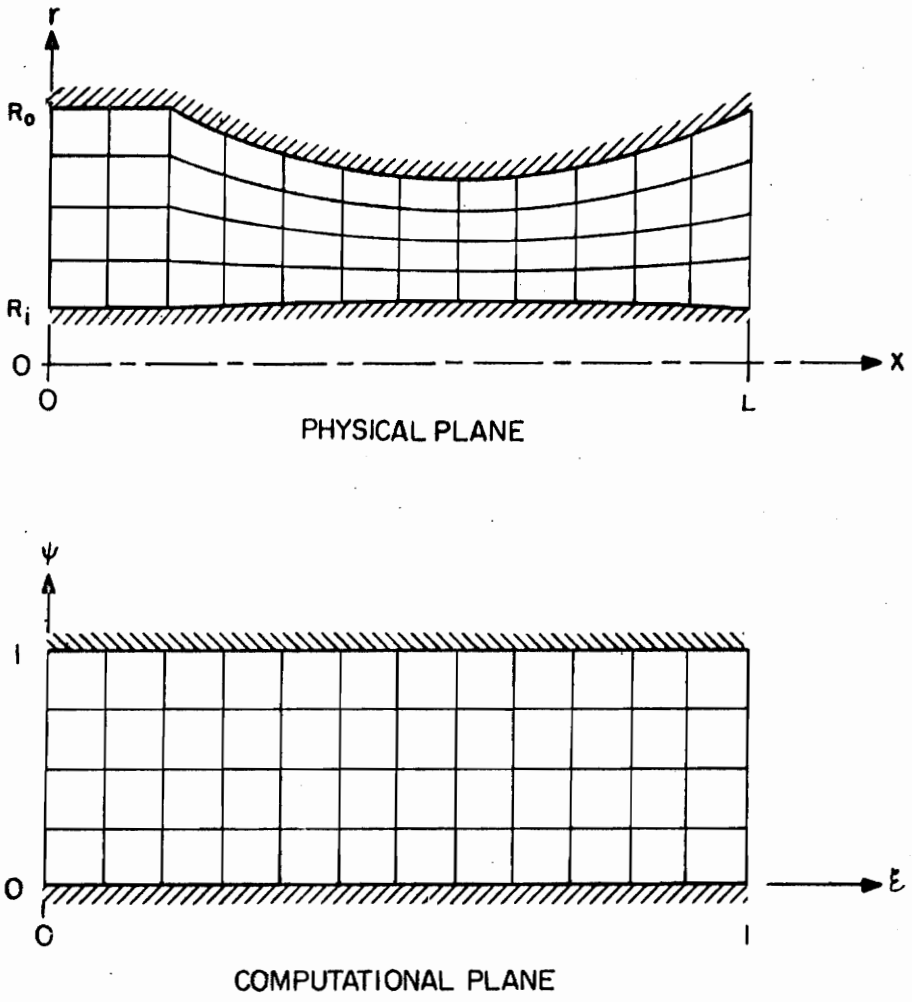

FIG. 1. COORDINATE TRANSFORMATION

The coordinate transformation used was:

$$\xi = \xi(x) = x/L$$

$$\psi = \psi(x,r) = \frac{r - R_i}{R_o - R_i} .$$

The derivatives of the velocity function and the rotation function can be transformed from the physical coordinates to the computational coordinates by application of the chain rule. These derivatives are:

$$\phi_x = \phi_\xi \, \xi_x + \phi_\psi \, \psi_x$$

$$\phi_r = \phi_\psi \, \psi_r$$

$$\phi_{xx} = \phi_{\xi\xi} \, \xi_x^2 + 2\phi_{\xi\psi} \, \xi_x \, \psi_x + \phi_{\psi\psi} \, \psi_x^2 + \phi_\psi \, \psi_{xx} + \phi_\xi \, \xi_{xx}$$

$$\phi_{rr} = \phi_{\psi\psi} \, \psi_r^2 + \phi_\psi \, \psi_{rr}$$

$$\phi_{xr} = \phi_{\xi\psi} \, \xi_x \, \psi_r + \phi_{\psi\psi} \, \psi_x \, \psi_r + \phi_\psi \, \psi_{xr}$$

$$F_x = F_\xi \, \xi_x + F_\psi \, \psi_x$$

$$F_r = F_\psi \, \psi_r$$

where

$$\xi_x = 1/L$$

$$\xi_{xx} = 0$$

$$\psi_x = -\frac{1}{R_o - R_i}\frac{dR_i}{dx} - \frac{r - R_i}{(R_o - R_i)^2}\left(\frac{dR_o}{dx} - \frac{dR_i}{dx}\right)$$

$$\psi_{xx} = -\frac{1}{R_o - R_i}\frac{d^2R_i}{dx^2} + \frac{2}{(R_o - R_i)^2}\frac{dR_i}{dx}\left(\frac{dR_o}{dx} - \frac{dR_i}{dx}\right)$$

$$- \frac{r - R_i}{(R_o - R_i)^2}\left(\frac{d^2R_o}{dx^2} - \frac{d^2R_i}{dx^2}\right) + 2\frac{r - R_i}{(R_o - R_i)^3}\left(\frac{dR_o}{dx} - \frac{dR_i}{dx}\right)^2$$

$$\psi_r = \frac{1}{R_o - R_i}$$

$$\psi_{rr} = 0$$

$$\psi_{rx} = -\frac{1}{(R_o - R_i)^2}\left[\frac{dR_o}{dx} - \frac{dR_i}{dx}\right].$$

Using these equations, Eq. 2.7 can be written in the quasi-linear form

$$A\,\phi_{\xi\xi} + B\,\phi_{\xi\psi} + C\,\phi_{\psi\psi} = D \tag{2.10}$$

where

$$A = \left[c^2 - (\phi_x + F)^2\right]\xi_x^2$$

$$B = 2\left[c^2 - (\phi_x + F)^2\right]\xi_x\,\psi_x - 2(\phi_x + F)\phi_r\,\xi_x\,\psi_r$$

$$C = \left[c^2 - (\phi_x + F)^2\right]\psi_x^2 + (c^2 - \phi_r^2)\,\psi_r^2$$

$$- 2(\phi_x + F)\,\phi_r\,\psi_x\,\psi_r$$

$$D = (\phi_x + F)\,\phi_r\,F_r - \frac{c^2}{r}\phi_r - \left[c^2 - (\phi_x + F)^2\right](F_x + \phi_\psi\,\psi_{xx})$$

$$+ 2(\phi_x + F)\,\phi_r\,\phi_\psi\,\psi_{xr}. \tag{2.11}$$

2.3 Finite Difference Approximation

The transformed governing equations were solved numerically using finite difference expressions to approximate the derivatives. To assure that the domain of dependence of the resulting algebraic equations matched that of the original partial differential equations, both centered and backward finite differences were used. The finite difference forms are presented in Table I. In the subsonic region all derivatives were evaluated by centered finite difference (second-order accurate) expressions. Radial derivatives in the supersonic region were also evaluated by centered differences, however, the axial derivatives (ϕ_ξ, $\phi_{\xi\xi}$, and F_ξ) were evaluated by backward finite differences with the first derivative expressions being second-order accurate and the second derivative expressions being only first-order accurate.

Steger (13) presents an example of the importance of using type-dependent finite difference expressions. He obtained a converged solution using type dependent finite differences. Then he changed the scheme so that centered finite differences were used everywhere. The solution remained stable until a small pertubation was introduced which caused the calculations to diverge.

TABLE I

FINITE DIFFERENCE EXPRESSIONS

Finite Difference Form	Type	Use
$\phi_\xi = \frac{\phi_{i+1,j} - \phi_{i-1,j}}{2\Delta\xi}$, $\phi_\psi = \frac{\phi_{i,j+1} - \phi_{i,j-1}}{2\Delta\psi}$	Centered	Subsonic axial and radial; Supersonic radial
$\phi_{\xi\xi} = \frac{\phi_{i+1,j} - 2\phi_{i,j} + \phi_{i-1,j}}{(\Delta\xi)^2}$, $\phi_{\psi\psi} = \frac{\phi_{i,j+1} - 2\phi_{i,j} + \phi_{i-1,j}}{(\Delta\psi)^2}$	Centered	Subsonic axial and radial; Supersonic radial
$\phi_{\xi\psi} = \frac{\phi_{i+1,j+1} - \phi_{i-1,j+1} - \phi_{i+1,j-1} + \phi_{i-1,j-1}}{4\Delta\xi\Delta\psi}$	Centered	Subsonic
$\phi_\xi = \frac{\phi_{i-2,j} - 4\phi_{i-1,j} + 3\phi_{i,j}}{2\Delta\xi}$	Backward	Supersonic axial
$\phi_{\xi\xi} = \frac{\phi_{i-2,j} - 2\phi_{i-1,j} + \phi_{i,j}}{(\Delta\xi)^2}$	Backward	Supersonic axial
$\phi_{\xi\psi} = \frac{\phi_{i-2,j+1} - 4\phi_{i-1,j+1} + 3\phi_{i,j+1} - \phi_{i-2,j-1} + 4\phi_{i-1,j-1} - 3\phi_{i,j-1}}{4\Delta\xi\Delta\psi}$	Backward	Supersonic

NOTE: See Fig. 2 for identification of subscripts.

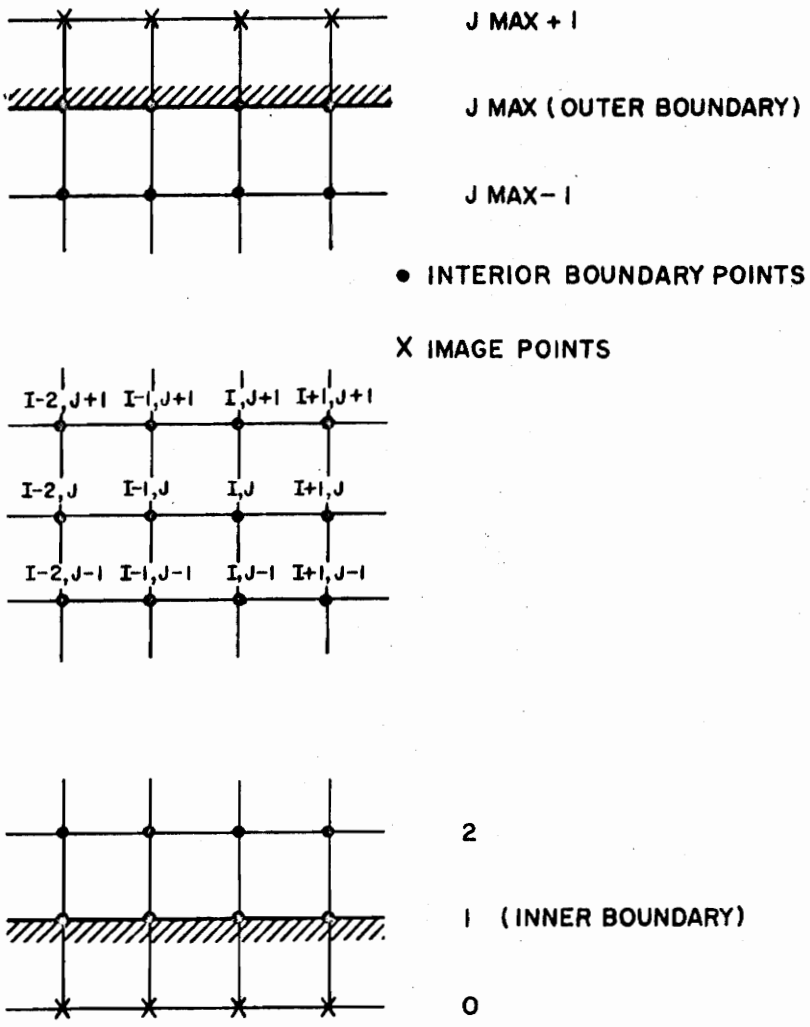

FIG. 2. MESH POINT NOMENCLATURE

2.4 Boundary Conditions

Proper boundary conditions must be applied to assure the existence of a unique solution of the governing equations. For the problem of transonic nozzle flow, conditions at the wall, inlet, and centerline (or centerbody) are required. Since only solutions with supersonic exit flow are desired, no exit boundary condition is required.

At the nozzle inlet a constant area section with walls parallel to the axis was added. At the beginning of this constant area section, the velocity function was set equal to a constant. This is equivalent to specifying zero radial velocity. Also, at this location the total pressure (either assumed or obtained from experiment) was specified as a function of radius.

For the application of boundary conditions at the walls, image points were established one mesh space past the walls, Fig. 2. The image points are denoted $\phi_{i,o}$ (center or inner wall) and $\phi_{i,jmax+1}$ (outer wall). The values of ϕ at these image points are specified such that the tangency condition

$$\frac{v}{u} = \frac{\phi_r}{\phi_x + F} = \frac{dR}{dx}$$

is met. In terms of the computational coordinates this becomes

$$\frac{\frac{\partial\phi}{\partial\psi}\frac{\partial\psi}{\partial r}}{\frac{\partial\phi}{\partial\xi}\frac{\partial\xi}{\partial x} + \frac{\partial\phi}{\partial\psi}\frac{\partial\psi}{\partial x} + F} = \frac{dR}{dx}$$

Rearrangement yields

$$\frac{\partial \phi}{\partial \psi} = \frac{dR}{dx}\left(\frac{\partial \phi}{\partial \xi}\frac{\partial \xi}{\partial x} + F\right) \Big/ \left(\frac{\partial \psi}{\partial r} - \frac{dR}{dx}\frac{\partial \psi}{\partial x}\right).$$

Application of centered finite differences permits solving for the values of the velocity function at the image points,

$$\phi_{i,jmax+1} = \phi_{i,jmax-1} + 2\Delta\psi \frac{\partial \phi}{\partial \psi}$$

$$\phi_{i,o} = \phi_{i,2} - 2\Delta\psi \frac{\partial \phi}{\partial \psi} .$$

Use of image points to satisfy the boundary conditions permits all points in the flow field to satisfy the governing equations.

Equation 2.7 requires special treatment at the centerline because it contains the indeterminate term, $\frac{\phi_r}{r}$. Application of l'Hospital's rule yields

$$\lim_{r \to 0} \frac{c^2}{r} \phi_r = c^2 \phi_{rr}.$$

Thus Eq. 2.7 reduces to

$$\left[c^2 - (\phi_x + F)^2\right](\phi_{xx} + F_x) + 2\, c^2\, \phi_{rr} = 0$$

at the centerline.

A boundary condition must be specified for F on some curve not tangent to the radial direction. This boundary condition does not affect the physical nature of the solution. Two boundary conditions were tested, one with F along the centerline equal to the axial velocity and the other with F along the center line equal to zero. These

boundary conditions produced slightly different results. However as mesh size was reduced the difference in results between the different specifications became smaller (see Section 3).

Further discussion of boundary conditions is presented in Section 6.2.

2.5 Relaxation Process

Upon introducing the finite difference operators discussed in Section 2.3, Eq. 2.10 takes the form

$$A\frac{\phi_{i-1,j} - 2\phi_{i,j} + \phi_{i+1,j}}{(\Delta\xi)^2} + B\frac{\phi_{i+1,j+1} - \phi_{i-1,j+1} - \phi_{i+1,j-1} + \phi_{i-1,j-1}}{4\Delta\xi\Delta\psi}$$

$$+ C\frac{\phi_{i,j-1} - 2\phi_{i,j} + \phi_{i,j+1}}{(\Delta\psi)^2} = D \qquad (2.12)$$

for subsonic flow. A similar equation is obtained for supersonic flow

$$A\frac{\phi_{i-2,j} - 2\phi_{i-1,j} + \phi_{i,j}}{(\Delta\xi)^2}$$

$$+ B\frac{\phi_{i-2,j+1} - 4\phi_{i-1,j+1} + 3\phi_{i,j+1} - \phi_{i-2,j-1} + 4\phi_{i-1,j-1} - 3\phi_{i,j-1}}{4\Delta\xi\Delta\psi}$$

$$+ C\frac{\phi_{i,j-1} - 2\phi_{i,j} + \phi_{i,j+1}}{(\Delta\psi)^2} = D. \qquad (2.13)$$

Values of A, B, C, and D are given as functions of ϕ by Eqs. 2.11. Considering just the i-th column, Eqs. 2.12 and 2.13 can be written

in matrix form

$$\tilde{A}_i\ (\phi)\ \tilde{\phi}_i = \tilde{f}(\phi) \quad .$$

where $\tilde{A}_i$ is a tridiagonal coefficient matrix containing the terms, A, B, and C; $\tilde{\phi}_i$ is the column vector of unknown ϕ's,

$$\tilde{\phi}_i = \begin{bmatrix} \phi_{i,1} \\ \phi_{i,2} \\ \cdot \\ \cdot \\ \cdot \\ \phi_{i,jmax-1} \\ \phi_{i,jmax} \end{bmatrix}$$

and $\tilde{f}$ is a column vector containing A, B, and D, values of ϕ upstream and downstream of the i-th column, and the image values $\phi_{i,jmax+1}$ and $\phi_{i,o}$. Thus both $\tilde{A}$ and $\tilde{f}$ are functions of ϕ.

Since the coefficient matrix $\tilde{A}$ is tridiagonal, the solution

$$\tilde{\phi}_i = \tilde{A}_i^{-1}\ \tilde{f} \tag{2.14}$$

can be obtained by the Thomas algorithm. The latest available values of ϕ are used to calculate $\tilde{A}$ and $\tilde{f}$. Then Eq. 2.14 is solved for $\tilde{\phi}_i$. Next, the underrelaxation relationship

$$\lambda\ \tilde{\phi}_i^{\ell+1} + (1 - \lambda)\ \tilde{\phi}_i^{\ell},$$

where λ is the column underrelaxation factor, is applied to these results, and the underrelaxed values are used to replace the ϕ values in

the i-th column. Then the values of ϕ at image points of the i-th column are calculated by the method described in the previous section.

This successive relaxation procedure is applied once to each column starting at the inlet and proceeding to the exit. After the last column has been reached, the relaxation relationship

$$\Lambda\ \phi_i^{\ell+1} + (1 - \Lambda)\ \phi_i^{\ell},$$

where Λ is the nozzle relaxation factor, is used to update all values of ϕ.

Two relaxation formulas are required to provide stability and fast convergence. The maximum value of λ for which the calculations were found to be stable is 0.7. In the subsonic region the value of Λ was determined according to Frankel (17) and varied from 1.0 to 2.0 depending on the mesh size. In the supersonic region the value of Λ was 0.9. Insufficient testing has been done to determine if these are the optimum values.

After updating all values of ϕ, F values are reevaluated. This is done by application of the relationship

$$F_r = \omega = \frac{M_o/u}{M_o\ \gamma\ P_o}\left(1 - \frac{\gamma-1}{2} M_o^{\,2}\right) \frac{\partial P_o}{\partial r},$$

which is repeated here from Eq. 2.8. Since F at the centerline or centerbody is known from the boundary conditions, F at any point in the flow field can be determined by integrating Eq. 2.8, using the trapezoidal rule,

$$F_{i,j} = F_{i,j-1} + \left(\frac{\omega_{i,j-1} + \omega_{i,j}}{2}\right)\frac{\Delta\psi}{\psi_r}.$$

The updated values of ϕ and F are used to recalculate the total pressure at each computational point. This procedure involves calculating the mass flow between the point at which the total pressure is to be determined and the centerbody or centerline. Then this mass flow is compared to the inlet mass flow to determine where the streamline crosses the inlet. Equation 2.9 implies that the total pressure is constant along a streamline, see Section 6.1.1. Thus the value of the total pressure at the inlet is equal to the total pressure at the downstream point in question. The total pressure at each mesh point at the inlet is known from the boundary data and linear interpolation is used to determine data between mesh points.

Based upon the new values of ϕ and F, values of ϕ at all image points are recalculated using the same procedure as previously described.

This relaxation procedure is repeated until the maximum change in Mach number for 100 iterations is less than some specified value, usually 0.001.

2.6 Special Computational Features of the Program

2.6.1 Mesh Halving

A method of mesh size halving similar to that of South and Jameson (11) was used to reduce computation time. A solution was first obtained with a coarse mesh such as 13 axial points by 6 radial points. A solution for this size mesh required very little computation time. Once the coarse mesh solution was obtained, the number of points in each direction was doubled to obtain a 25 x 11 mesh. Initially straight-line

interpolation was used to determine the values of ϕ, F, and P_o at the intermediate points. However it was found that this procedure did not give results with smooth variations in velocity. Therefore a parabolic interpolation procedure was used. The equation for interpolating ϕ at a point which does not lie near a boundary was

$$\phi_{i,j} = (-\phi_{i-3,j} + 9\phi_{i-1,j} + 9\phi_{i+1,j} - \phi_{i+3,j})/16.$$

Near the inlet (i=2) the special relationship

$$\phi_{i,j} = (3\phi_{i-1,j} + 6\phi_{i+1,j} - \phi_{i-3,j})/8.$$

was used. Similar equations were used at the other boundaries. This solution was then used as the initial solution for the refined mesh.

The mesh halving procedure can be repeated as often as desired until the array space is exceeded. Typically a solution starts with a 13 x 6 mesh, proceeds to a 25 x 11 mesh, and ends with a 49 x 21 mesh.

2.6.2 Input-Output Features

Subroutines were added to the program to provide some special input and output features. These include the ability to handle arbitary nozzle shape, to compute lines of constant Mach number, and to compute the discharge coefficient.

Coordinates of any nozzle geometry may be specified in the data deck. Values of the radii at mesh points are determined by a spline fit of the input data. The spline fit subroutines also supply the first and second derivatives of the wall radii. Thus the value of the wall slope at a certain point does not depend upon the computational mesh size.

For output purposes lines of constant Mach number are determined by linearly interpolating the calculated Mach numbers and the coordinates of the grid points. Flow angles along the lines of constant Mach number are also computed by linear interpolation.

The discharge coefficient is obtained by dividing the actual mass flow by the mass flow determined from one-dimensional theory based on the mass flow weighted average total pressure. The equations for these evaluations are:

$$\overline{P_o} = \frac{\int P_o \, \rho (2\pi r \, dr)}{\int \rho \, 2\pi r \, dr}$$

$$C_D = \frac{\int \rho \, 2\pi r \, dr}{\rho^* V^* \pi (R_o^{*2} - R_i^{*2})}$$

where ρ^*, V^*, R_o^*, and R_i^* are sonic values based on $\overline{P_o}$ and one-dimensional theory. The integrations were carried out by use of the trapezoidal rule.

3. RESULTS

The procedure described in the preceding sections was coded in Fortran IV for an IBM 370/158 computer (see Section 6.3 for flow chart). The coding was given the acronym RETIRE (RElaxation of Transonic Flows Including Rotational Effects). Three nozzle geometries were tested, a hyperbolic nozzle, a convergent-divergent nozzle similar to a case run by Wehofer and Moger (6), and a typical fan bypass nozzle of a modern turbofan engine. These geometries are shown in Fig. 3. All cases were run with and without total pressure gradients.

Typical computational times for some of the test cases are shown in Table II. The computational times are larger than would normally be expected for relaxation methods. However, the present version of the program is in a research form, and computational efficiency has not yet been optimized.

In Fig. 4, lines of constant Mach number for the hyperbolic nozzle with uniform inlet flow are compared with the results obtained by Oswatitsch and Rothstein (18) using series expansion methods. Agreement between the two methods is good. The figure also shows results for two mesh sizes, a 25 x 11 mesh and a 49 x 21 mesh. The similarity of results indicates the lack of dependence of the solution on mesh size.

As would be expected, the accuracy of the solution is dependent upon the mesh size. Since the finite difference form governing equations which the program solves are not in conservative form (see Murman (19) and Roache (20) for a discussion of conservative form), the solution of the equations does not exactly obey conservation of

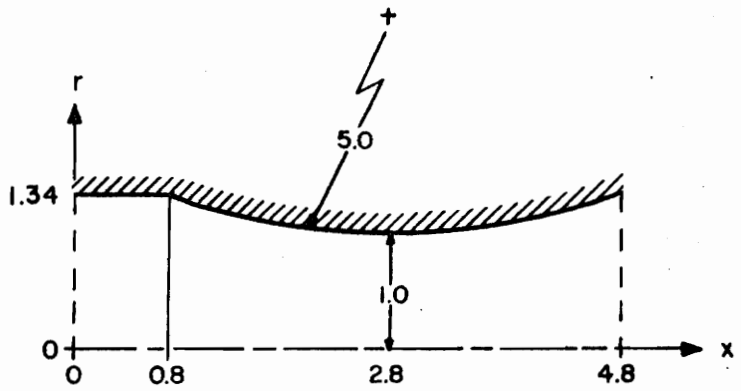

(a) HYPERBOLIC NOZZLE

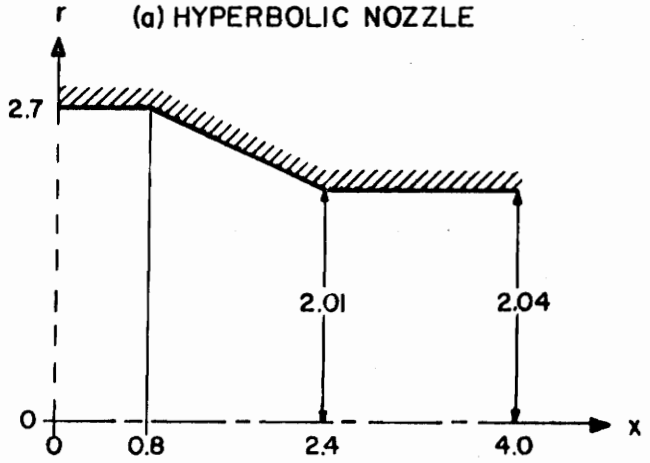

(b) WEHOFER & MOGER NOZZLE

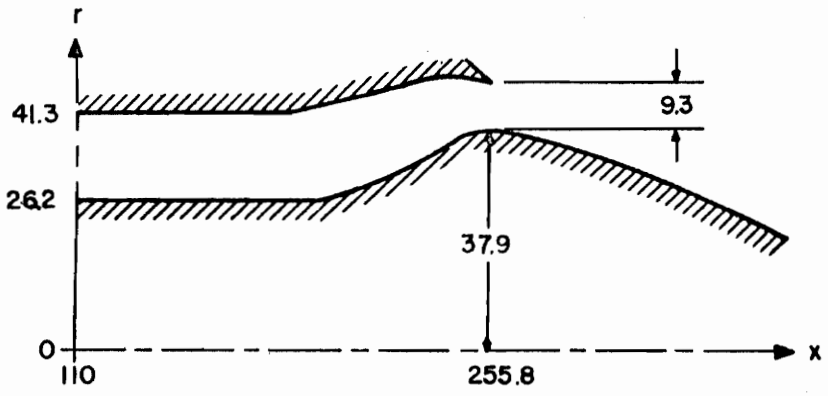

(c) TURBOFAN BYPASS DUCT (NOT TO SCALE)

FIG. 3. NOZZLE GEOMETRIES (ALL DIMENSIONS IN INCHES)

TABLE II

TYPICAL COMPUTATION TIMES

Case	Inlet	Mesh	No. of Iterations	Computation Time (Sec)	Time Per Point (Sec)	Normalized Times Per Point* (Sec)
Hyperbolic	Uniform	13 x 6	100	27	0.35	0.12
		25 x 11	300	234	0.85	0.28
		49 x 21	700	1740	1.69	0.56
	Nonuniform	13 x 6	700	155	1.98	0.66
		25 x 11	1300	667	2.43	0.81
		49 x 21	1800	2344	2.28	0.76
Wehofer & Moger	Nonuniform	14 x 11	400	187	1.21	0.40
		27 x 21	900	1143	2.02	0.67
Turbofan Bypass Nozzle	Uniform	13 x 6	200	51	0.65	0.22
		25 x 11	600	423	1.54	0.51
	Nonuniform	13 x 6	1500	395	5.06	1.89
		25 x 11	1800	685	2.50	0.83

*Normalized with respect to an IBM 370/165 for comparison with (1).

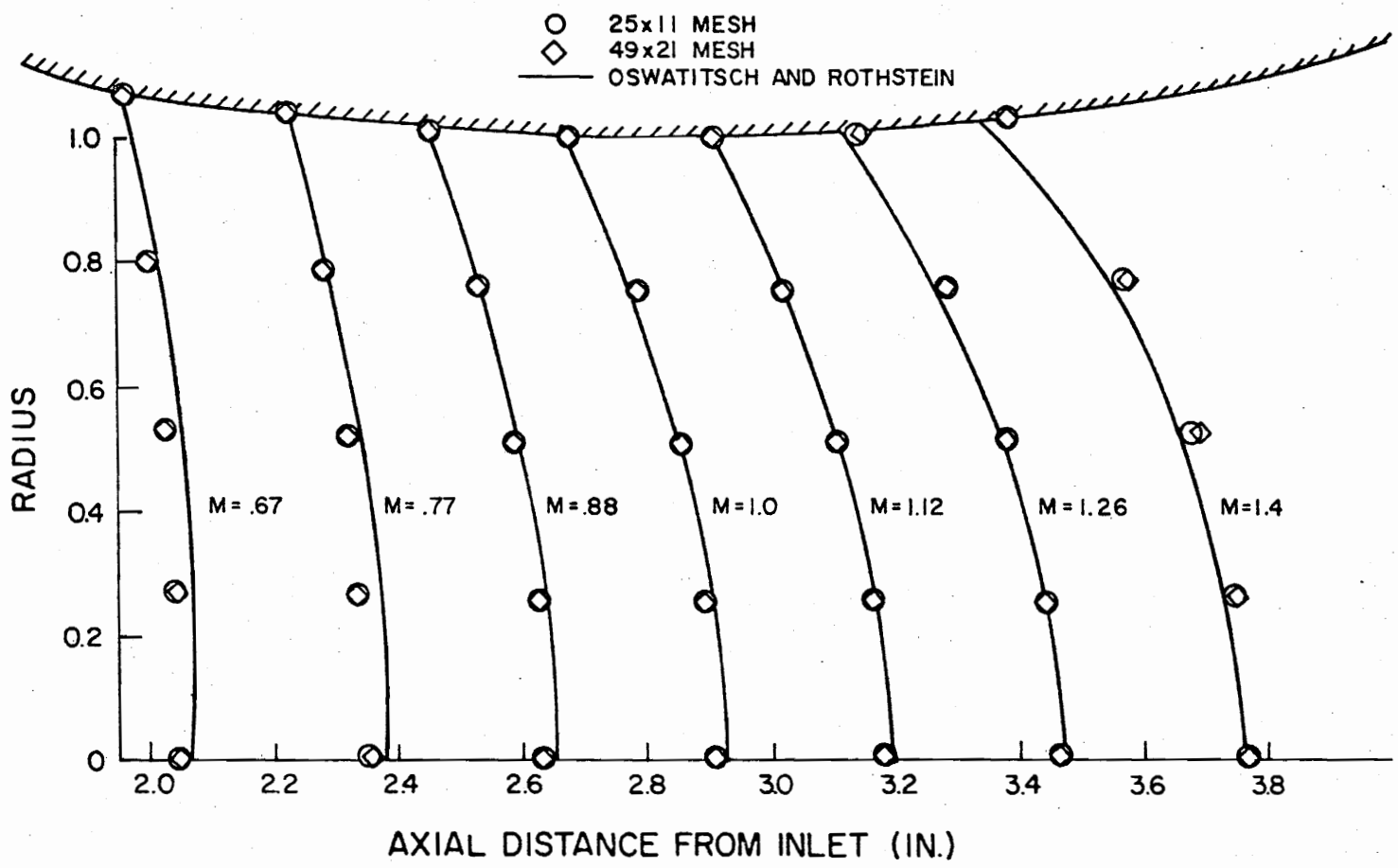

FIG. 4. HYPERBOLIC NOZZLE — LINES OF CONSTANT MACH NUMBER (UNIFORM FLOW)

mass. The calculated mass flow at one axial location might be slightly different from the calculated mass flow at another axial location. However as the mesh size is reduced, the accuracy of the solution improves and the variation in the calculated mass flow decreases. Variations in discharge coefficient, (a measure of mass flow) with axial position can be viewed as an indication of the accuracy of the solution. It is seen in Fig. 5 that as the mesh spacing is reduced, the discharge coefficient approaches a constant value. This implies that a fine mesh results in a more accurate solution to the original partial differential equations than obtained with a coarse mesh. At the throat, the computed value of discharge coefficient does not vary with mesh size. Therefore the discharge coefficient calculated at the throat can be considered to be an accurate prediction of the discharge coefficient of the nozzle regardless of mesh spacing.

Also illustrated in Fig. 5 are the effects on discharge coefficient of two different specifications of F at the centerline. In one case the centerline values of F are zero at all axial positions. In the other case, the centerline values of F are set equal to the axial velocities. The latter specification resulted in a reduced discharge coefficient variation and a more accurate solution.

Figure 6 shows the effect of a total pressure gradient on isomach lines for a hyperbolic nozzle. A 25% variation in the total pressure caused a significant shift in the lines of constant Mach number and a 1% decrease in discharge coefficient. In this case, the effects of total pressure gradient on the discharge coefficient were greater than the effects of two-dimensionality, which caused a 0.2% decrease in dis-

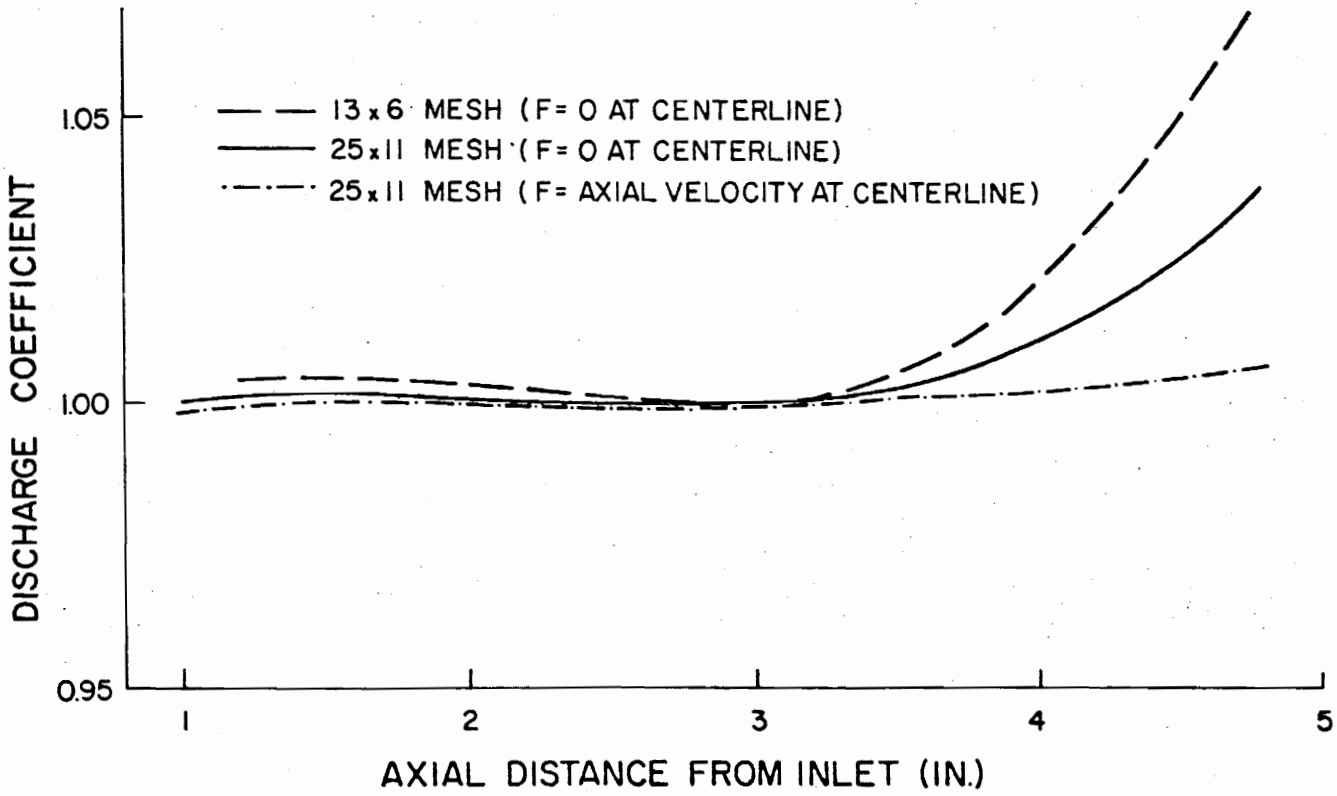

FIG. 5. DISCHARGE COEFFICIENT FOR HYPERBOLIC NOZZLE (UNIFORM FLOW)

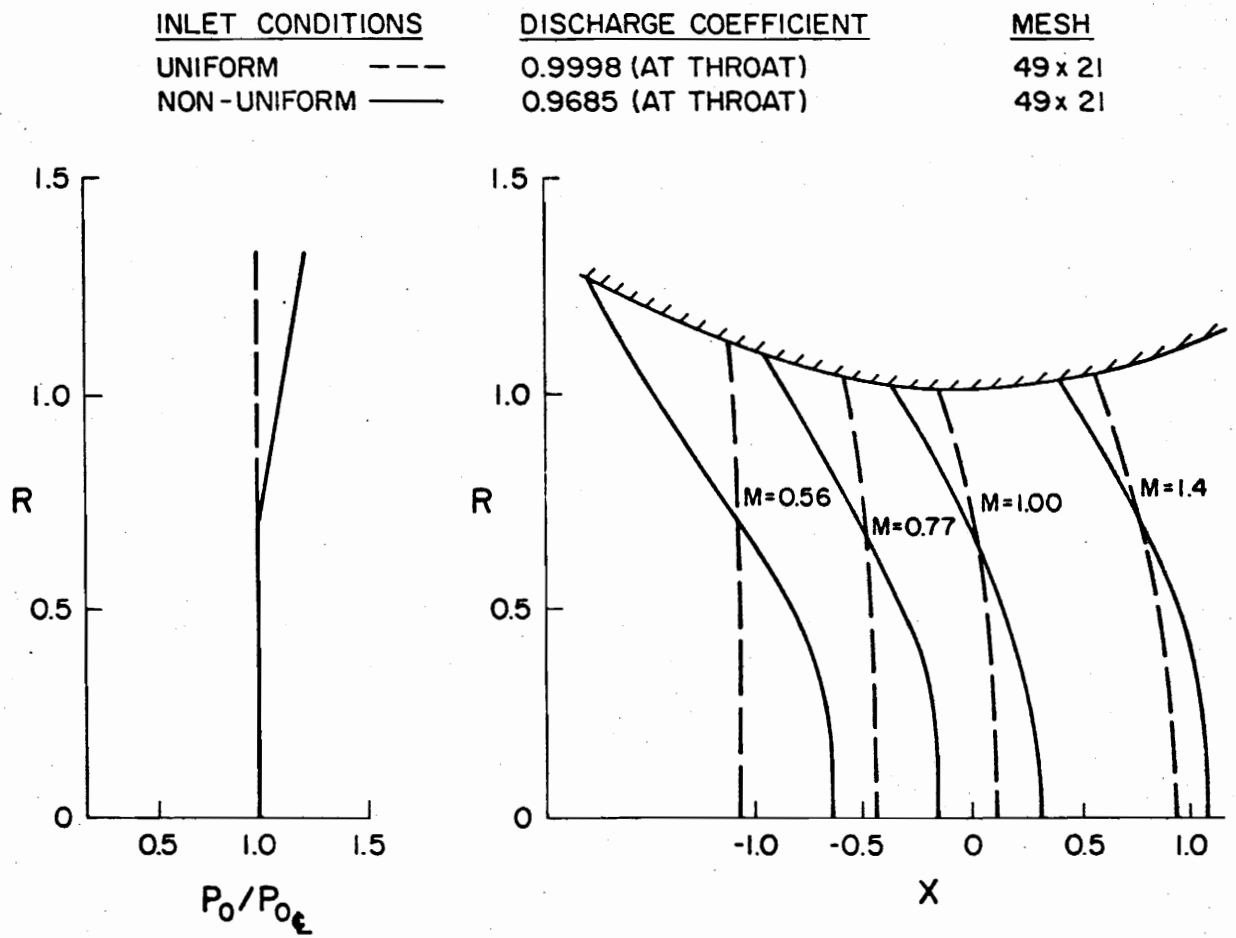

INLET TOTAL PRESSURE (X = -2.80)

LINES OF CONSTANT MACH NUMBER

FIG. 6. HYPERBOLIC NOZZLE

charge coefficient.

There are very few analytical solutions for the effects of nonuniform inlet flows available for comparison with the present calculations. Ferri and Dash (5) consider a convergent-divergent nozzle with nonuniform inlet flow. However, because of uncertainties in their use of boundary conditions and in their treatment of viscosity and heat transfer, the results are unsuitable for comparison. Wehofer and Moger used a time dependent method to obtain a solution for nozzles with nonuniform inlet flow. At present they have published the results of only one convergent-divergent nozzle calculation.* The same nozzle was run with the present program. Figure 7 shows that the results of the RETIRE program agree well with the analytical and experimental results. The discharge coefficient calculated by Wehofer and Moger included a boundary layer correction. Since RETIRE does not include a boundary layer correction, a discharge coefficient slightly higher than either Wehofer and Moger's analytical value or their experimental value is to be expected.

In all fairness it must be admitted that the results shown in Fig. 7 are not conclusive proof of the accuracy of the present program in handling nonuniform inlet flows. This is because there is only a 6% variation in total pressure, and therefore the results of nonuniform inlet flow differ only slightly from the uniform inlet flow results.

---

*Because of the lack of experimental data, a test program was conducted at the Arnold Engineering Development Center to obtain experimental results to enable additional comparisons with Wehofer and Moger's calculation to be made. The results of some of this work have been reported in Wehofer and Matz (2) but the bulk of the data is as yet unpublished.

CASE	DISCHARGE COEFFICIENT	MESH
WEHOFER & MOGER ——	0.95 (WITH B.L. CORRECTION)	UNKNOWN
PRESENT SOLUTION – – –	0.97 (AT THROAT)	27 x 21
EXPERIMENTAL ●	0.96	—

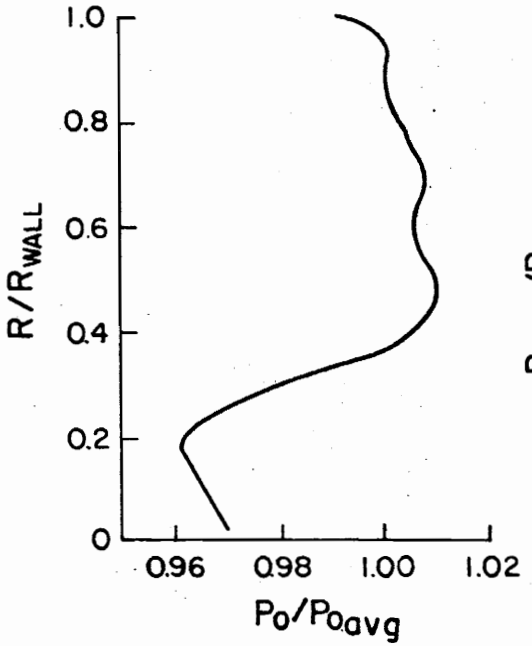

INLET TOTAL PRESSURE
(X = -2.47)

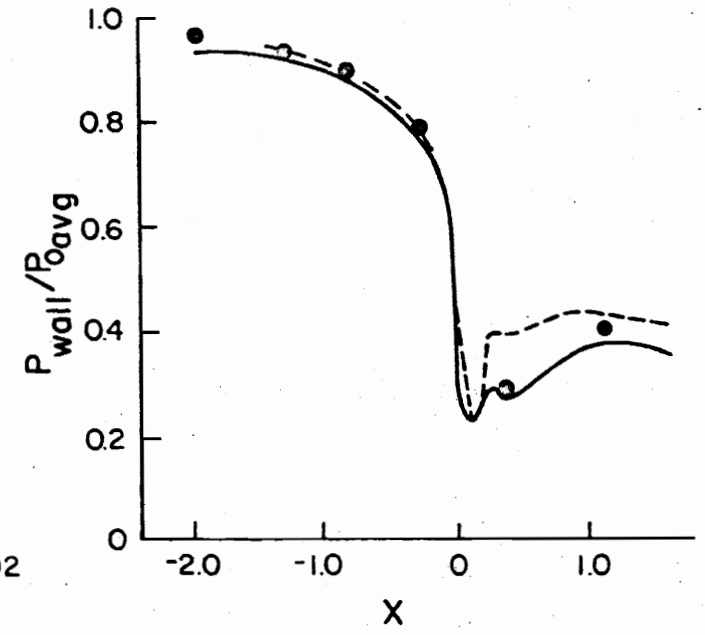

WALL STATIC PRESSURE VARIATION

FIG. 7. TURBOFAN EXHAUST NOZZLE

For example, the discharge coefficient for uniform flow was 0.972 compared to 0.974 for nonuniform inlet flow, the maximum difference in wall static pressure between the two results was only about 1%.

Therefore, a final test case was run which clearly shows the effect of inlet flow rotation. A case was selected which would demonstrate this effect in an actual turbofan aircraft nozzle. For this purpose a typical fan bypass nozzle was chosen, and inlet total pressure variations typical for such nozzles were used. Two modifications of the original data were required to render it suitable for input to the present program:

1. Because the original nozzle had an insufficient divergent section to produce supersonic flow at the exit, as required by the present version of the program, a divergent section was added as shown by the dashed lines in Fig. 8.
2. Since wall values of the total pressure were not supplied, values were chosen as indicated by the dashed lines in the left portion of this figure. The particular extrapolation used was chosen to provide a sufficiently large velocity at the inner and outer walls.

Figure 8 shows that the total pressure gradient resulted in a large shift in the lines of constant Mach number and a 1% decrease in the discharge coefficient. This clearly demonstrates that in this case of actual aircraft application the effects of inlet flow nonuniformities cannot be neglected.

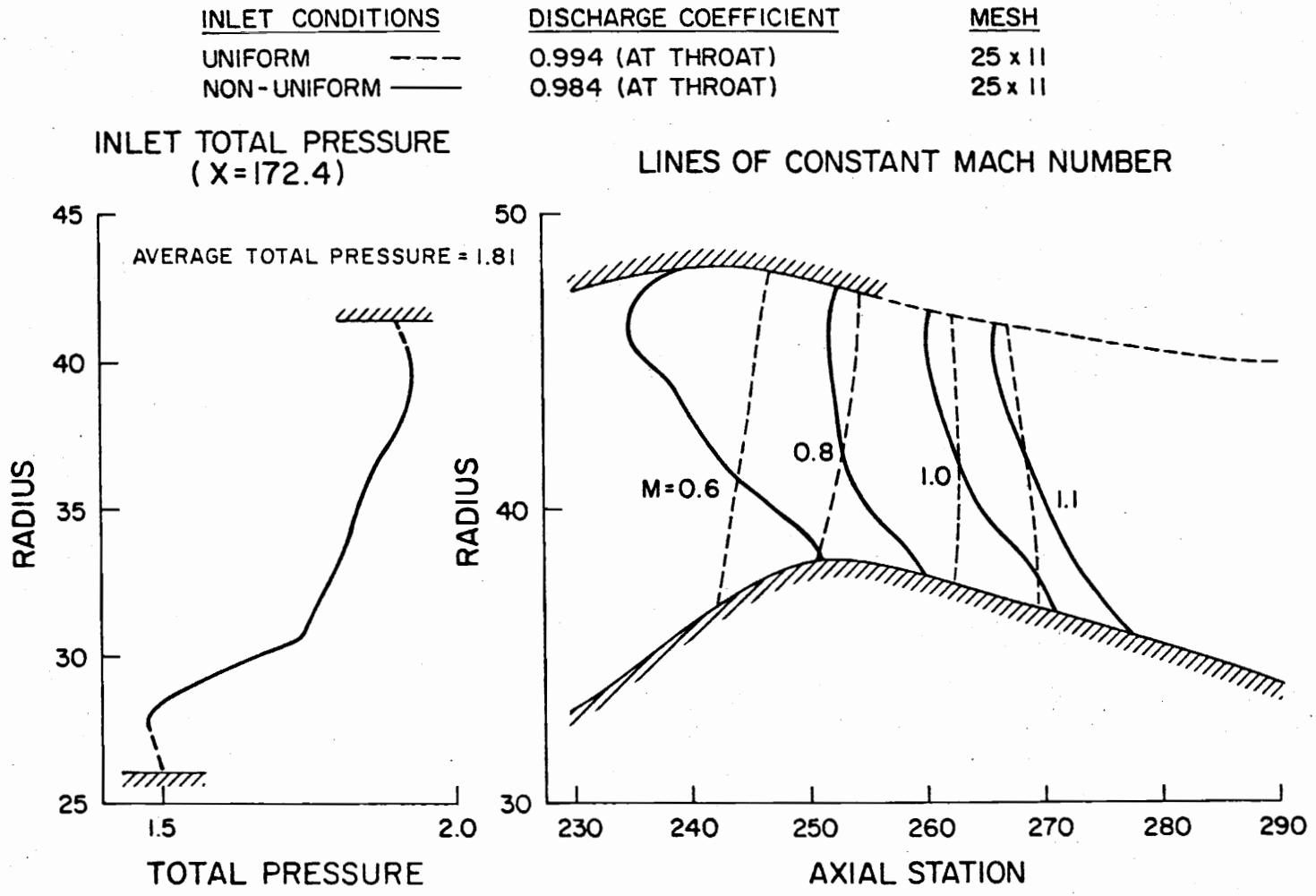

FIG. 8. TURBOFAN BYPASS DUCT

4. CONCLUSIONS

This work was successful in demonstrating the feasibility, accuracy, and importance of including the effects of total pressure gradients in evaluating propulsion nozzle performance. In fact, in the cases considered here inlet flow nonuniformities produced effects greater than those which resulted from a consideration of just the two-dimensionality of the flow. For the hyperbolic nozzle and the turbofan bypass nozzle, two-dimensional effects were found to produce a reduction in discharge coefficient of only 0.1 to 0.6%. Whereas, nonuniform inlet flow effects produced an additional decrease in the discharge coefficient of about 1%.

Agreement with the solutions of Oswatitsch and Rothstein (18) and Wehofer and Moger (6) is good. However, available experimental data does not provide conclusive proof of the program's accuracy. It is expected that more test data will soon be available from tests conducted by Wehofer and Matz at the Arnold Engineering Development Center. Also, more experimental data is available for nozzles with subsonic exhausts and for convergent nozzles (2). When, as recommended in the next section, the capability of handling subsonic exit flow and convergent nozzles is incorporated into the program, further comparison to experimental data will be possible.

5. RECOMMENDATIONS

The present program is in what may be considered a research form. Therefore, this section presents some recommendations for improving the present program by increasing its flexibility and its computational speed.

Since total temperature gradients do not affect the Mach number distribution within the nozzle, consideration of these gradients was not contained in the program development. This does not imply that significant total temperature gradients do not exist in an actual propulsion nozzle. Nor does it imply that these gradients do not affect nozzle performance coefficients such as discharge coefficient and thrust coefficient. At a specified Mach number and total pressure, both density and velocity are influenced by the total temperature. In fact, Wehofer and Matz have shown that typical total temperature gradients have a significant effect on nozzle performance. The effects can be evaluated after a converged solution which ignores the existence of total temperature gradients is obtained. Appropriate subroutines to accomplish this should be added to the program.

Because the program is in a research form, little effort was made to reduce computation time or to provide a program which could easily be used by those not familiar with its operation. From previous experience it is expected that by removing unnecessary operations and optimizing the relaxation factors, computational time could be halved. The input and output features should be improved to increase the ease of operation of the program. Error messages should be added to identify

conditions which the program cannot handle such as strong shocks (shocks at Mach number greater than 1.3) and unsuitable nozzle geometry.

In its present form, the program requires that the flow at the nozzle exit be completely supersonic. However, most of the nozzles used on today's aircraft are simple convergent nozzles where the exit flow at most is mixed (partially subsonic and partially supersonic). Therefore, the program should be modified to include the capability to evaluate the performance of convergent nozzles. This requires that the character of the jet plume be calculated. This is of importance not only because it is necessary to predict nozzle performance but also because the exhaust plume affects aircraft performance due to the interation of the plume with the fuselage and wings.

Another factor influencing aircraft performance is the effect which the forward motion of the aircraft produces on the configuration of the jet and therefore on nozzle performance. To include this external flow effect two streams of different total pressure must be considered. Neglecting viscosity, a slip stream would exist between the two streams. To account for the differences in total pressure across the slip stream, a discontinuity in F could be specified. Then it may be possible to solve the whole flow field using the same basic procedures which were discussed previously.

6. APPENDIX

6.1 Derivation of Governing Equations

6.1.1 Preliminary Considerations

Certain preliminary facts and relationships will have to be established for the development of the governing equations. The first of these is that for flow of a chemically homogeneous substance, in the absence of heat conduction, body forces, viscosity, shocks, and shaft work (see Chapman and Walker (21)), entropy is constant along a streamline. Also, under the above assumptions the first law of thermodynamics implies that total enthalpy is constant along a streamline. If for a pure substance both the entropy and total enthalpy are constant along a streamline, the stagnation state of the fluid cannot change along a streamline. In particular total pressure and total temperature are constant along streamlines.

It will be necessary to have an equation which permits the rotation to be evaluated from measurable properties. According to Crocco's Theorem (4)

$$\omega = \frac{1}{V}\left(\frac{\partial h_o}{\partial n} - T\,\frac{\partial S}{\partial n}\right) \tag{6.1}$$

where the rotation ω is defined by

$$\omega \equiv \frac{\partial u}{\partial r} - \frac{\partial v}{\partial x}\,.$$

A basic thermodynamic relationship involving entropy is

$$T\,dS = dh - \frac{1}{\rho}\,dP,$$

from which it follows that

$$T_o \frac{\partial S_o}{\partial n} = \frac{\partial h_o}{\partial n} - \frac{1}{\rho_o}\frac{\partial P_o}{\partial n}\,. \tag{6.2}$$

Since by the definition of the stagnation state, $S_o = S$, combining Eqs. 6.1 and 6.2 gives

$$\omega = \frac{1}{V}\left[\frac{\partial h_o}{\partial n} - \frac{T}{T_o}\left(\frac{\partial h_o}{\partial n} - \frac{1}{\rho_o}\,\frac{\partial P_o}{\partial n}\right)\right]. \tag{6.3}$$

From conservation of energy

$$\frac{T}{T_o} = 1 - \frac{\gamma-1}{2} M_o^2.$$

Introducing this into Eq. 6.3 gives

$$\omega = \frac{1}{V}\left[\frac{\partial h_o}{\partial n} - \left(1 - \frac{\gamma-1}{2} M_o^2\right)\left(\frac{\partial h_o}{\partial n} - \frac{1}{\rho_o}\,\frac{\partial P_o}{\partial n}\right)\right].$$

Using the following perfect gas (ideal gas, constant specific heats) relationships

$$V = M_o \sqrt{\gamma R T_o}\,,$$

$$\frac{\partial h_o}{\partial n} = C_p \frac{\partial T_o}{\partial n}\,,$$

and

$$C_p = \frac{\gamma R}{\gamma-1}$$

yields

$$\omega = \frac{1}{M_o\sqrt{\gamma R T_o}} \left[\frac{\gamma R M_o^2}{2} \frac{\partial T_o}{\partial n} + \left(1 - \frac{\gamma-1}{2} M_o^2 \right) \frac{1}{\rho_o} \frac{\partial P_o}{\partial n} \right]. \tag{6.4}$$

Since measurements of stagnation conditions are normally conducted in the x-r coordinate system it is necessary to convert this equation from the streamline coordinate system to the x-r coordinate system. This is done by application of the chain rule and the previously discussed fact that total pressure and total temperature are constant along streamlines. Therefore,

$$\frac{\partial T_o}{\partial s} = \frac{\partial T_o}{\partial x} \frac{\partial x}{\partial s} + \frac{\partial T_o}{\partial r} \frac{\partial r}{\partial s} = 0 \tag{6.5}$$

and

$$\frac{\partial T_o}{\partial n} = \frac{\partial T_o}{\partial x} \frac{\partial x}{\partial n} + \frac{\partial T_o}{\partial r} \frac{\partial r}{\partial n} . \tag{6.6}$$

Applying the coordinate transformation equations

$$\frac{\partial r}{\partial s} = \frac{v}{V} \qquad \frac{\partial x}{\partial s} = \frac{u}{V}$$

$$\frac{\partial r}{\partial n} = \frac{u}{V} \qquad \frac{\partial x}{\partial n} = - \frac{v}{V}$$

to Eq. 6.5 yields

$$\frac{\partial T_o}{\partial x} = - \frac{v}{u} \frac{\partial T_o}{\partial r} . \tag{6.7}$$

Substituting into Eq. 6.6 yields

$$\frac{\partial T_o}{\partial n} = \frac{V}{u} \frac{\partial T_o}{\partial r} .$$

Likewise for total pressure

$$\frac{\partial P_o}{\partial n} = \frac{V}{u} \frac{\partial P_o}{\partial r} .$$

Thus Eq. 6.4 becomes

$$\omega = \frac{V/u}{M_o\sqrt{\gamma R\, T_o}} \left[\frac{\gamma R\, M_o}{2} \frac{\partial T_o}{\partial r} + \left(1 - \frac{\gamma-1}{2} M_o^2 \right) \frac{1}{\rho_o} \frac{\partial P_o}{\partial r} \right]. \tag{6.8}$$

It is convenient to nondimensionalize all variables in this equation with respect to the stagnation speed of sound (c_o) and the radius of the outer wall at the throat (R_{th}). Accordingly, the following relationships are employed:

$$\hat{u} \equiv \frac{u}{c_o} = \frac{u}{\sqrt{\gamma R T_o}}$$

$$\hat{v} \equiv \frac{v}{c_o} = \frac{v}{\sqrt{\gamma R T_o}}$$

$$\hat{x} \equiv \frac{x}{R_{th}}$$

$$\hat{r} \equiv \frac{r}{R_{th}} .$$

From the definition of rotation

$$\omega \equiv \frac{\partial u}{\partial r} - \frac{\partial v}{\partial x} = \frac{1}{R_{th}} \left[\frac{\partial (\hat{u}\sqrt{\gamma R\, T_o})}{\partial \hat{r}} - \frac{\partial (\hat{v}\sqrt{\gamma R\, T_o}}{\partial \hat{x}} \right].$$

Expanding and using Eq. 6.7 yields

$$\omega = \frac{1}{2R_{th}} \sqrt{\frac{\gamma R}{T_o}} \left[2T_o \left(\frac{\partial \hat{u}}{\partial \hat{r}} - \frac{\partial \hat{v}}{\partial \hat{x}} \right) + \frac{M_o^2}{\hat{u}} \frac{\partial T_o}{\partial \hat{r}} \right]. \tag{6.9}$$

Equating the right hand sides of Eq. 6.8 and Eq. 6.9 yields after simplification

$$2T_o\left(\frac{\partial \hat{u}}{\partial \hat{r}} - \frac{\partial \hat{v}}{\partial \hat{x}}\right) + \frac{M_o^2}{\hat{u}} \frac{\partial T_o}{\partial \hat{r}}$$

$$= \frac{1}{\hat{u}}\left[M_o^2 \frac{\partial T_o}{\partial \hat{r}} + \frac{2}{\gamma}\left(1 - \frac{\gamma-1}{2} M_o^2\right)\frac{T_o}{P_o}\frac{\partial P_o}{\partial \hat{r}}\right]$$

or

$$\frac{\partial \hat{u}}{\partial \hat{r}} - \frac{\partial \hat{v}}{\partial \hat{x}} = \left(1 - \frac{\gamma-1}{2} M_o^2\right)\frac{1}{\gamma P_o}\frac{\partial P_o}{\partial \hat{r}} .$$

Now since

$$\hat{\omega} \equiv \frac{\partial \hat{u}}{\partial \hat{r}} - \frac{\partial \hat{v}}{\partial \hat{x}}$$

then

$$\hat{\omega} = \left(1 - \frac{\gamma-1}{2} M_o^2\right)\frac{1}{\gamma P_o} \frac{\partial P_o}{\partial \hat{r}} . \qquad (6.10)$$

6.1.2 Velocity Equation

In cylindrical coordinates the continuity equation (22) for steady flow is

$$\frac{1}{r}\frac{\partial}{\partial r}(r\rho v) + \frac{1}{r}\frac{\partial}{\partial \theta}(\rho w) + \frac{\partial}{\partial x}(\rho u) = 0.$$

For axisymmetric flow

$$w = 0$$

$$\frac{\partial}{\partial \theta} = 0$$

which permits the simplified continuity equation

$$\frac{1}{r}\frac{\partial}{\partial r}(r\rho v) + \frac{\partial}{\partial x}(\rho u) = 0$$

to be written. Expanding gives

$$u\frac{\partial \rho}{\partial x} + v\frac{\partial \rho}{\partial r} + \rho\left(\frac{\partial u}{\partial x} + \frac{\partial v}{\partial r} + \frac{v}{r}\right) = 0. \tag{6.11}$$

Examining the first two terms of this equation, it can be noted that

$$u\frac{\partial \rho}{\partial x} + v\frac{\partial \rho}{\partial r} = \frac{D\rho}{Dt}$$

for steady flow. Since density can be expressed as a function of pressure and entropy, the chain rule yields,

$$\frac{D\rho}{Dt} = \frac{\partial \rho}{\partial P}\bigg|_S \frac{DP}{Dt} + \frac{\partial \rho}{\partial S}\bigg|_P \frac{DS}{Dt}\,. \tag{6.12}$$

However, because entropy is constant along a streamline $\frac{DS}{Dt}$ is zero. Noting that the sonic speed is defined by the equation

$$c^2 \equiv \frac{\partial P}{\partial \rho}\bigg|_S\,,$$

Eq. 6.12 can be reduced to

$$\frac{D\rho}{Dt} = \frac{1}{c^2}\frac{DP}{Dt}\,. \tag{6.13}$$

Euler's equation for isentropic flow along a streamline,

$$dP = -\rho\frac{dV^2}{2}\,,$$

yields

$$\frac{DP}{Dt} = -\frac{\rho}{2}\frac{DV^2}{Dt} .$$

Therefore Eq. 6.13 becomes

$$\frac{D\rho}{Dt} = -\frac{\rho}{2c^2}\frac{DV^2}{Dt} .$$

Expressing this equation in terms of the velocity components results in

$$\frac{D\rho}{Dt} = -\frac{\rho}{c^2}\left[u^2\frac{\partial u}{\partial x} + v^2\frac{\partial v}{\partial r} + uv\left(\frac{\partial u}{\partial r} + \frac{\partial v}{\partial x}\right)\right] .$$

Substituting this into Eq. 6.11 and rearranging gives

$$(c^2 - u^2)\frac{\partial u}{\partial x} + (c^2 - v^2)\frac{\partial v}{\partial r} - uv\left(\frac{\partial u}{\partial r} + \frac{\partial v}{\partial x}\right) + \frac{c^2 v}{r} = 0.$$

Using the same procedure as in the previous section, this equation can be nondimensionalized. This gives

$$(\hat{c}^2 - \hat{u}^2)\frac{\partial \hat{u}}{\partial \hat{x}} + (\hat{c}^2 - \hat{v}^2)\frac{\partial \hat{v}}{\partial \hat{r}} - \hat{u}\hat{v}\left(\frac{\partial \hat{u}}{\partial \hat{r}} + \frac{\partial \hat{v}}{\partial \hat{x}}\right) + \frac{\hat{c}^2\hat{v}}{\hat{r}}$$

$$+ \frac{R_{th}}{c_o^2}(\hat{c}^2 - M_o^2)\left(u\frac{\partial c_o}{\partial x} + v\frac{\partial c_o}{\partial r}\right) = 0 \qquad (6.14)$$

where

$$\hat{c}^2 \equiv \frac{c^2}{c_o^2} = 1 - \frac{\gamma-1}{2}M_o^2 .$$

Examining the last term of Eq. 6.14 yields

$$u\frac{\partial c_o}{\partial x} + v\frac{\partial c_o}{\partial r} = \frac{Dc_o}{Dt}$$

for steady flow. The substantial derivative is the rate of change of a property for a fluid particle as it moves along a streamline. However, it was shown that all stagnation properties are constant along streamlines. Therefore

$$\frac{D\, c_o}{Dt} = 0.$$

Equation 6.14 reduces to

$$(\hat{c}^2 - \hat{u}^2)\frac{\partial \hat{u}}{\partial \hat{x}} + (\hat{c}^2 - \hat{v}^2)\frac{\partial \hat{v}}{\partial \hat{r}} - \hat{u}\hat{v}\left(\frac{\partial \hat{u}}{\partial \hat{r}} + \frac{\partial \hat{v}}{\partial \hat{x}}\right) + \frac{\hat{c}^2\hat{v}}{\hat{r}} = 0. \tag{6.15}$$

Let ϕ, G, and F be functions such that

$$\phi_{\hat{x}} + F \equiv \hat{u} \tag{6.16}$$

$$\phi_{\hat{r}} + G \equiv \hat{v}. \tag{6.17}$$

By differentiating Eq. 6.16 by $\hat{r}$ and Eq. 6.17 by $\hat{x}$ and subtracting the results, it can be shown that

$$F_{\hat{r}} - G_{\hat{x}} = \hat{\omega}.$$

Substituting Eqs. 6.16 and 6.17 into Eq. 6.15 yields

$$\left[\hat{c}^2 - (\phi_{\hat{x}} + F)\right](\phi_{\hat{x}\hat{x}} + F_{\hat{x}}) + \left[\hat{c}^2 - (\phi_{\hat{r}} + G)^2\right](\phi_{\hat{r}\hat{r}} + G_{\hat{r}}) - (\phi_{\hat{x}} + F)(\phi_{\hat{r}} + G)(2\phi_{\hat{x}\hat{r}} + F_{\hat{r}} + G_{\hat{x}}) + \hat{c}^2\frac{(\phi_{\hat{r}} + G)}{\hat{r}} = 0.$$

For notational simplicity, the circumflexes (^) were dropped from the equations in the preceding sections of this report.

6.2 A Note on Boundary Conditions

A discussion of boundary conditions applicable to inflow and outflow boundaries for the problem of steady inviscid compressible flow with total pressure gradients is presented in this section. The governing equations for this problem can be cast in many forms as discussed in Section 1.3. In spite of the form of the equations, the basic problem is unchanged; and similar boundary conditions are applicable to any form of the governing equations; but the ease of applying a particular boundary condition is dependent on the form of the governing equations. The particular form of the governing equations considered in the following discussion will be the same as developed previously.

Two types of problems are of importance; namely subsonic flow at both the inlet and exit and subsonic inflow with supersonic outflow. In either case one acceptable, but not sufficient, boundary condition is the specification of the total pressure along some curve not tangent to the characteristic directions of Eq. 2.9, i.e., not tangent to a streamline. Since the inlet of the nozzle is such a curve, specification of total pressure along the nozzle inlet as a function of radius is always acceptable.

The remaining boundary conditions involve the velocity components or ϕ and F. For the purpose of illustrating the proper boundary conditions analogies will be made to similar problems and to a simplified form of the governing equations of Section 2.1. It will be assumed

that the total pressure is uniform at the inlet; and since F is then zero at all points, Eq. 2.7 reduces to the potential equation

$$(c^2 - \phi_x^2)\phi_{xx} + (c^2 - \phi_r^2)\phi_{rr} - 2\phi_x \phi_r \phi_{xr} + \frac{c^2}{r}\phi_r = 0.$$

With completely subsonic flow, the potential equation is elliptic and applicable boundary conditions are similar to those appropriate for Laplace's equation

$$\nabla^2\phi = 0.$$

There are two classical types of boundary conditions for Laplace's equation, Neumann and Dirichlet.

The Neumann boundary condition is the specification of the normal derivative of ϕ at all boundaries. However the existence of a solution to the Neumann problem is conditional in that the integral of the normal derivative of ϕ over the boundary must be zero (23). A physical illustration of this condition comes from consideration of steady incompressible flow for which the governing equation is Laplace's equation. Thus the Neumann problem for incompressible flow only has a solution if the total inflow equals the total outflow. This is simply a statement of the conservation of mass.

For the compressible flow problem, it would be expected that the existence of a solution would be conditional if Neumann boundary data were given. Specifying ϕ_x at both the inlet and exit is equivalent to specifying the mass flow at both places. Unless the mass flows were consistent, no solution would exist. A complication arises in that the

mass flows would not necessarily be equal. It is seen in Fig. 5 that a slight error is introduced into the solution by the finite mesh size. Thus for the numerical solution the mass flow at the inlet is not exactly equal to the mass flow at the exit. The effect of slight inconsistencies in mass flow specifications on computational stability is not known.

An alternate specification of the boundary conditions is the Dirichlet problem where ϕ in Laplace's equation is specified along the boundaries. There are no conditions on the existence of a solution of the Dirichlet problem. Thus application of Dirichlet data to the inflow and outflow boundaries of the nozzle flow problem should result in a well-posed problem. If a constant area section is added to each end of the nozzle, ϕ can be specified as a different constant at each end. This is equivalent to specifying zero radial velocities at the inlet and exit. The average velocity in the nozzle would be proportional to the difference between ϕ at the inlet and exit. Therefore use of Dirichlet data appears to be an acceptable way to pose the subsonic flow problem. The appropriateness of these boundary conditions is not affected by regions of supersonic flow within the nozzle. The criterion for determining appropriate inlet and exit boundary conditions involves only the nature of the flow at these boundaries.

The next type of problem considered is nozzle flow with a subsonic inlet and a supersonic exit. Since the flow is subsonic at the inlet the previous discussion is still applicable for the inlet. However, an additional difficulty arises with the use of the Neumann boundary condition since a knowledge of the mass flow is required before a

solution can be obtained. For a choked nozzle this value is unique and unknown before the calculations are carried out. Thus Neumann data cannot be used for a choked nozzle and Dirichlet data would be the natural alternative.

At the exit boundary the governing equations are hyperbolic, and applicable boundary conditions are similar to those appropriate for the wave equation

$$\frac{\partial^2 \phi}{\partial x^2} - \frac{\partial^2 \phi}{\partial r^2} = 0.$$

The classical problem for the wave equation is the Cauchy problem where the ϕ and ϕ_r would be specified at r=0 and no other boundary data would be required. Thus by analogy with the nozzle flow problem no boundary data should be specified at the exit. This is consistent with the principle that flow conditions at a downstream point cannot influence an upstream point in supersonic flow.

Similar conclusions were derived by Ganz and Serra (24) through an energy integral method and by Gopalakrishman and Bozzola (25) through an analysis of the characteristics of the governing equations. The governing equations were in forms different from those considered here, but as mentioned previously this does not affect the applicability of their conclusions.

6.3 Flow Chart

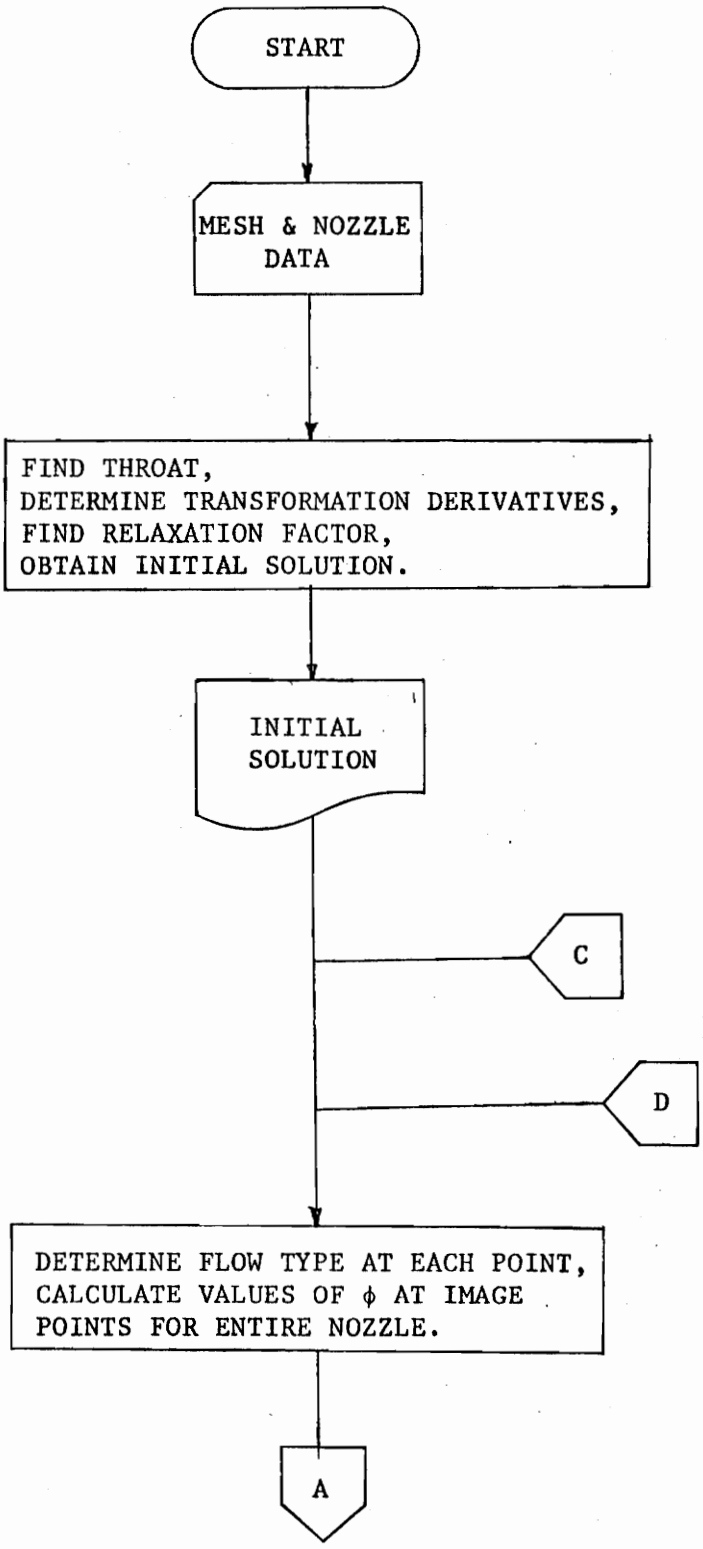

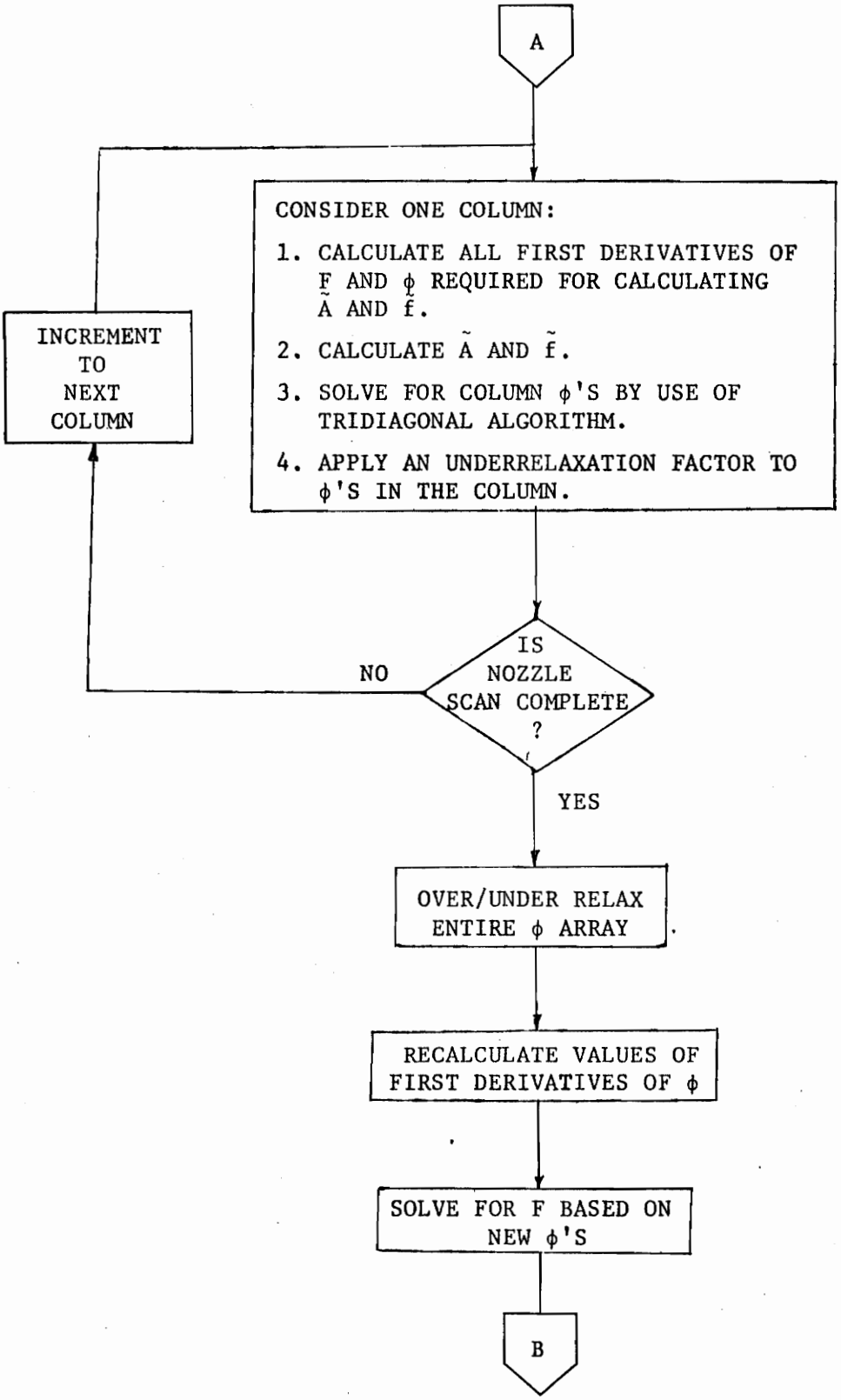
A
CONSIDER ONE COLUMN:
1. CALCULATE ALL FIRST DERIVATIVES OF F AND φ REQUIRED FOR CALCULATING Ã AND f̃.
2. CALCULATE Ã AND f̃.
3. SOLVE FOR COLUMN φ'S BY USE OF TRIDIAGONAL ALGORITHM.
4. APPLY AN UNDERRELAXATION FACTOR TO φ'S IN THE COLUMN.
INCREMENT TO NEXT COLUMN
IS NOZZLE SCAN COMPLETE ?
NO
YES
OVER/UNDER RELAX ENTIRE φ ARRAY
RECALCULATE VALUES OF FIRST DERIVATIVES OF φ
SOLVE FOR F BASED ON NEW φ'S
B

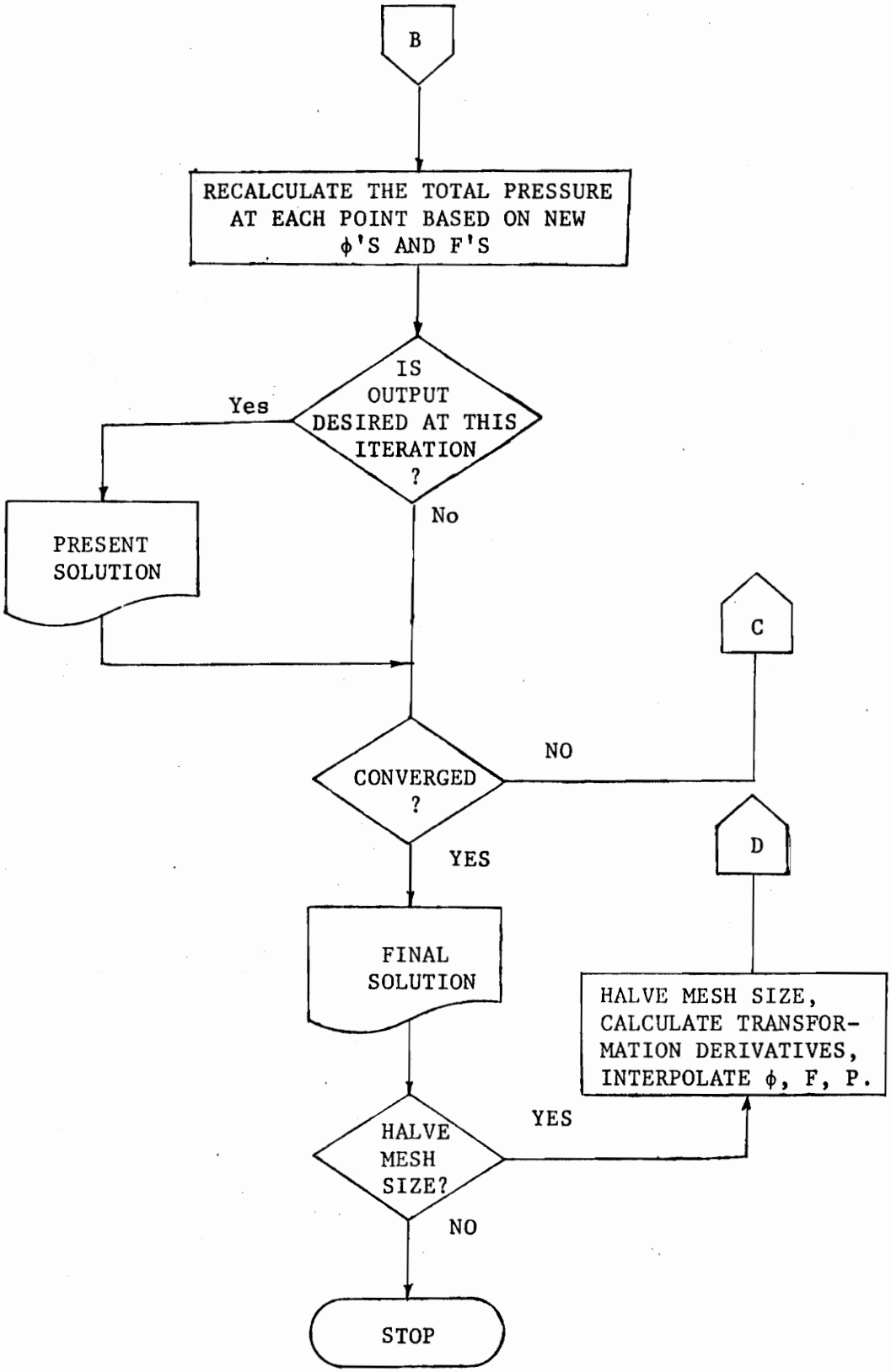
B
RECALCULATE THE TOTAL PRESSURE AT EACH POINT BASED ON NEW ϕ'S AND F'S
IS OUTPUT DESIRED AT THIS ITERATION ?
Yes
No
PRESENT SOLUTION
C
CONVERGED ?
NO
YES
D
FINAL SOLUTION
HALVE MESH SIZE, CALCULATE TRANSFORMATION DERIVATIVES, INTERPOLATE ϕ, F, P.
HALVE MESH SIZE?
YES
NO
STOP

7. REFERENCES

1. Brown, E. F., "Transonic Nozzle Flow: A Critical Survey of Analytical Methods," Douglas Aircraft Company, Report MDC J6223, September, 1973.

2. Wehofer, S., and R. J. Matz, "Turbine Engine Exhaust Nozzle Performance," AIAA Paper No. 73-1302, 1973.

3. Walsh, Kevin E., "An Application of Relaxation Methods to Transonic Nozzle Flow," Master's Thesis, Mechanical Engineering Department, Virginia Polytechnic Institute and State University, Blacksburg, Virginia, September, 1974.

4. Shapiro, A. H., The Dynamics and Thermodynamics of Compressible Fluid Flow, Ronald Press Co., New York, 1953, p. 282.

5. Ferri, A., and S. Dash, "The Calculation of Nozzle Discharge Coefficients Accounting for Viscosity Losses and Flow Nonuniformities," Advanced Technology Laboratories, Inc., Jericho, New York, Report ATL TR 160, October, 1970.

6. Wehofer, S., and W. C. Moger, "Analysis and Computer Program for Evaluation of Airbreathing Propulstion Exhaust Nozzle Performance," ARO, Inc., Arnold Airforce Station, Tennessee, AEDC-TR-73-29.

7. Wehofer, S., and W. C. Moger, "Transonic Flow in Conical Convergent and Convergent-Divergent Nozzles with Nonuniform Inlet Conditions," AIAA Paper No. 70-635, 1970.

8. Emmons, Howard W., "The Numerical Solution of Compressible Fluid Flow Problems," NACA Technical Note No. 932, 1944.

9. Murman, E. M., and J. D. Cole, "Calculation of Plane Steady Transonic Flows," AIAA Paper No. 70-188, 1970.

10. Jameson, A., "Numerical Calculations of the Three Dimensional Transonic Flow Over a Yawed Wing," Proceedings AIAA Computational Fluid Dynamics Conference, 1973, pp. 18-26.

11. South, J. C., Jr., and A. Jameson, "Relaxation Solutions for Inviscid Axisymetric Transonic Flow Over Blunt or Pointed Bodies," Proceedings AIAA Computational Fluid Dynamics Conference, 1973, pp. 8-17.

12. Bailey, F. R., and J. L. Steger, "Relaxation Techniques for Three-Dimensional Transonic Flow About Wings," AIAA Paper No. 72-189, 1972.

13. Steger, J. L., "Application of Cyclic Relaxation Procedures to Transonic Nozzle Flow Fields," Ph.D. Dissertation, Iowa State University, Ames, Iowa, 1969.

14. Steger, J. L., Ames Research Center, NASA, Moffett Field, California, private communication.

15. Taulbee, D. B., and S. Boraas, "Transonic Nozzle Flow with Non-uniform Total Energy," AIAA Journal, October, 1971, Vol. 9, No. 10, pp. 2102-2104.

16. Roache, P. J., Computational Fluid Dynamics, Hermosa Publishers, Albuquerque, New Mexico, 1972, pp. 290-301.

17. Roache, p. 118.

18. Oswatitsch, K., and W. Rothstein, "Flow Patterns in a Converging-Diverging Nozzle," NACA Tech. Memo. No. 1215, 1949.

19. Murman, E. M., "Computational Methods for Inviscid Transonic Flows with Imbedded Shock Waves," Flight Sciences Laboratory, Boeing Scientific Research Laboratories, February, 1971, p. 45.

20. Roache, pp. 11, 28-33.

21. Chapman, A. J., and W. F. Walker, Introductory Gas Dynamics, Holt, Rinehart, and Winston, Inc., New York, 1971, pp. 347-348.

22. Shames, I. H., Mechanics of Fluids, McGraw-Hill Book Company, New York, 1962.

23. Chester, C. R., Techniques in Partial Differential Equations, McGraw-Hill Book Company, New York, 1971, p. 71.

24. Ganz, A. A., and R. A. Serra, "Boundary Conditions and Uniqueness in Internal Gas Dynamic Flows," AIAA Journal, Vol. 12, No. 3, March, 1974, pp. 263-264.

25. Gopalakrishnan, S. and R. Bozzola, "Numerical Representation of Inlet and Exit Boundary Conditions in Transonic Cascade Flow," ASME Paper No. 73-GT-55, 1973.

8. VITA

The author was born on January 18, 1952 in Huntington, West Virginia. He attended school in Cincinnati, Ohio where he graduated from Woodard High School in June, 1970.

In September, 1970 he entered Virginia Polytechnic Institute. During 1971 he participated in the Cooperative Education Program, working six months for the Norfolk Naval Shipyard. Between 1973 and 1974 he worked six months for the General Electric Company. He obtained a Bachelor of Science degree in Mechanical Engineering in June, 1974, and began graduate study in September of that year toward a Master of Science degree in Mechanical Engineering.

The author is a member of Pi Tau Sigma and the American Society of Mechanical Engineers, and is registered as an Engineer-in-Training in Virginia.

Thoralf Brecht

Thoralf Brecht

A RELAXATION METHOD FOR THE SOLUTION OF ROTATIONAL TRANSONIC NOZZLE FLOW

by

Thoralf Brecht

(ABSTRACT)

Relaxation methods have been used for several years for the solution of isentropic external flow. Recently, successive line relaxation was applied to solve the problem of isentropic transonic flow of an ideal gas in a convergent-divergent nozzle. However, measurements of total temperature and total pressure indicate that the flow in a turbofan nozzle is rotational and not isentropic. Definition of a new function similar to the potential function allows the successive line relaxation techniques to be applied to rotational nozzle flows.

Test cases show good agreement with the time dependent calculations and experimental results. A test case of a typical turbofan bypass nozzle indicates a 1% decrease in discharge coefficient because of total pressure gradients.